Simulated acid mine drainage treatment in iron oxidizing ceramic membrane bioreactor with subsequent co-precipitation of iron and arsenic

Emir Kasım Demir[1], Belma Nural Yaman[2], Pınar Aytar Çelik[3], Jaakko A. Puhakka[4], Erkan Sahinkaya[1,5*]

[1]*Environmental and Energy Systems Engineering Program, Istanbul Medeniyet University, Istanbul, 34700, Turkey*

[2] *Department of Biomedical Engineering, Eskisehir Osmangazi University, Eskisehir, 26040, Turkey*

[3]*Environmental Protection and Control Program, Eskisehir Osmangazi University, Eskisehir, 26110, Turkey*

[4]*Tampere University, Faculty of Engineering and Natural Sciences, P.O. Box 541, FI-33104 Tampere University, Finland*

[5]*Department of Bioengineering, Istanbul Medeniyet University, Istanbul, 34700, Turkey*

* Corresponding author: erkan.sahinkaya@medeniyet.edu.tr

Abstract

Acid mine drainage (AMD), generated in the active and abandoned mine sites, is characterized by low pH and high metal concentrations. One AMD treatment possibility is biologically oxidizing Fe^{2+} followed by precipitation through pH control. As compared to autotrophic iron oxidizing microbial community, a microbial community enriched in the presence of organic nutrients was hypothesized to yield higher biomass during commissioning the bioreactor. In this study, the treatment of Fe, Cu, Co, Mn, Zn, Ni, and As containing simulated AMD was studied using an iron-oxidizing ceramic membrane bioreactor (CMBR) at varying hydraulic retention times (HRTs) (6-24 h) and two different feed Fe^{2+} concentrations (250 and 750 mg/L). The impact of tryptone soya broth (TSB) on the CMBR performance was also investigated. Almost complete Fe^{2+} oxidation and sustainable flux at around 5.0 L/(m^2.h) were obtained in the CMBR with the *Alicyclobacillus tolerans* and *Acidiphilium cryptum* dominated enrichment culture. The Fe^{2+} oxidation rate, as assessed in batch operation cycles of CMBR, increased significantly with increasing Fe^{2+} loading to the bioreactor. The iron oxidation rate decreased by the elimination of organic matter from the feed. The increase of the CMBR permeate pH to 3.5-4.0 resulted in selective co-precipitation of As and Fe (over 99%) with the generation of biogenic schwertmannite.

Keywords: Iron oxidation; Acid mine drainage; Arsenic removal; Schwertmannite; Ceramic Membrane Bioreactor; *Alicyclobacillus tolerans*

1. Introduction

Acid mine drainage (AMD) generated during the mining operations degrades the environment for long-term durations. The dissolution of the sulfide-bearing metallic wastes is hazardous to adjacent water resources (Natarajan, 2008). The main sources of AMD are waste tailings, underground and open-cast mines, stockpiles, and spent heap leach dumps (Natarajan, 2008). Among the metal-sulfides, pyrite (FeS_2) is the main mineral responsible for the AMD

generation as its bio-oxidation may be quite fast when exposed to water and air (Kefeni et al., 2017). AMD causes severe environmental problems due to its low pH, high concentration of toxic heavy metals, metalloids, and sulfate (Aytar et al., 2015; Blodau, 2006; Kefeni et al., 2017). Ferrous iron is bio-oxidized to ferric iron forming iron-oxide precipitates, known as a yellow boy (reactions 1-3) (Kefeni et al., 2017). In general, *Acidithiobacillus ferrooxidans* and *Acidithiobacillus thiooxidans* are responsible for generating AMD (Natarajan, 2008).

$$FeS_2 + 7/2O_2 + H_2O \rightarrow Fe^{2+} + 2SO_4^{2-} + 2H^+ \quad \text{(R-1)}$$

$$Fe^{2+} + ¼\ O_2 + H^+ \rightarrow Fe^{3+} + ½\ H_2O \quad \text{(R-2)}$$

$$Fe^{3+} + 3H_2O \rightarrow Fe(OH)_3 + 3H^+ \quad \text{(R-3)}$$

The overall reaction may be summarized as follows (Johnson and Hallberg, 2005).

$$4FeS_2 + 15O_2 + 14H_2O \rightarrow 4Fe(OH)_3 + 8SO_4^{2-} + 16H^+ \quad \text{(R-4)}$$

Once formed, the Fe^{3+} is used for pyrite dissolution even in the absence of oxygen according to the following faster reaction (Kefeni et al., 2017).

$$FeS_2 + 14Fe^{3+} + 8H_2O \rightarrow 15Fe^{2+} + 2SO_4^{2-} + 16H^+ \quad \text{(R-5)}$$

Arsenic is one of the common contaminants in AMD (Casiot et al., 2003) and deserves special attention due to its high toxicity and carcinogenicity (Bissen et al., 2003). Arsenopyrite decomposition may occur according to the following reaction (R-6) and Fe^{3+} generated by iron-oxidizing bacteria, such as *Acidithiobacillus ferrooxidans*, increases arsenopyrite oxidation according to R-7 (Natarajan, 2008).

$$FeAsS + 3.5O_2 + H_2O \rightarrow Fe^{3+} + SO_4^{2-} + H_2AsO_4^- \quad \text{(R-6)}$$

$$FeAsS + 13Fe^{3+} + 8H_2O \rightarrow 14Fe^{2+} + SO_4^{2-} + 13H^+ + H_3AsO_4 \quad \text{(R-7)}$$

In addition to bioleaching, active iron-oxidizing bioprocesses can also be used for AMD treatment (Demir et al., 2020; Rowe and Johnson, 2008). For this purpose, many types of bioreactors have been used including fluidized bed reactors (FBR) (Ozkaya et al., 2007), biological jarosite carrier-based biofilms (Ahoranta et al., 2020), packed-bed bioreactors (Rowe and Johnson, 2008), a modular continuous flow bioreactor (Hedrich and Johnson, 2012), serially connected tank reactors filled with suspended biofilm carriers (Sandström and Mattsson, 2001), and even membrane bioreactors (Demir et al., 2020; Park et al., 2005). Conventional active chemical treatment (e.g. lime addition, aeration, and precipitation of metal hydroxides at pH 7-8.5) may have generate voluminous and poorly settleable sludge (Hedrich and Johnson, 2012) and result in high operational costs associated with high dosages of chemicals. AMD contains iron, arsenic, and many other precious heavy metals, i.e. Cu and Zn. Hence, the removal of non-precious iron together with toxic arsenic (Ahoranta et al., 2016) may increase the possibility of recovering precious heavy metals from AMD and decreases the treatment and sludge handling cost. In this context, Hedrich & Johnson (2012) used a modular continuous bioreactor system for iron oxidation in the first reactor inoculated with autotrophic *Ferrovum myxofaciens*, selective iron precipitation as schwertmannite at pH 3.5 in the second reactor and a third packed bed polishing bioreactor after which soluble iron decreased to < 1 mg/L. The modular system selectively removed iron from a synthetic AMD containing Al, Cu, Mn, and Zn. In another study, Ahoranta et al. (2016) investigated iron oxidation in an FBR and simultaneous removal of ferric iron and arsenic in a gravity settler connected to the FBR. They achieved high Fe^{2+} (5 g/L) oxidation and As(III) (10 mg/L) removals (> 99%) at pH 3.0 due to adsorption and co-precipitation with biogenic jarosite. Selective arsenic and iron separation from valuable metal solution during bioleaching has also been reported (Wakeman et al., 2011).

AMD treatment research has focused on uses of autotrophic iron-oxidizing bacteria, such as *Acidithiobacillus ferrooxidans*. However, many heterotrophic and mixotrophic bacteria oxidize ferrous iron (Rowe and Johnson, 2008). High efficiency of iron oxidation depends on the quantity of bacteria retained in the bioreactor. However, reaching high quantity of autotrophic iron-oxidizers may be slow due to low energy gain from the oxidation of iron (Rowe and Johnson, 2008), especially at low concentrations. Hence, the use of organic nutrient supplementation may be advantageous, especially, during the initial commissioning of the bioprocess due to higher growth yield of heterotrophs/mixotrophs compared to autotrophic counterparts (Demir et al., 2020; Rowe and Johnson, 2008).

Several studies have reported the use of biofilm reactors for iron oxidation (Ahoranta et al., 2020; Özkaya et al., 2007; Sandström and Mattsson, 2001), whilst membrane bioreactors (MBRs) to retain iron oxidizing acidophiles have rarely been used (Demir et al., 2020; Park et al., 2005). Some microorganisms may not attach to the media present in biofilm reactors. Hence, the process performance may completely depend on the attachment performance of the culture on the selected media. Also, it may be difficult to aerate and achieve proper hydraulic conditions in some biofilm reactors. Hence, MBRs, which have deserved significant attention in recent years for wastewater treatment (Huang and Lee, 2015), may also be used as an alternative to biofilm reactors for iron oxidation. In our previous study (Demir et al., 2020), efficiency of ceramic MBR (CMBR) for iron oxidation in the presence of an organic compound was demonstrated. However, the presence of metals often encountered in AMD, e.g. Cu, Co, Mn, Zn, Ni, and As, on the process performance has not been investigated.

This study aims at investigating the performance of a CMBR at varying hydraulic retention times (HRTs) and membrane fluxes for iron oxidation in a synthetic (containing Fe, Cu, Co, Mn, Zn, Ni, and As) AMD. The CMBR performance was also tested in the presence and absence of an organic matter. Further, dynamic changes of bacterial community in the CMBR

was investigated. Also, the selective precipitation of iron and arsenic in the CMBR permeate as schwertmannite at pHs 3.0-4.0 was investigated.

2. Materials and Methods

2.1. Ceramic Membrane Bioreactor and the Composition of Synthetic AMD

The CMBR was operated previously (Demir et al., 2020) in the presence of ferrous iron (~ 1400 mg/L) and tryptone soya broth (TSB, 250 mg/L) at pH 1.5-2.5 for 205 days. The details about the bioreactor were presented in Demir et al. (2020). Briefly, the bioreactor had a total and working volumes of 4.7 L and 3.0 L, respectively. The pore size of the ceramic flat-sheet membrane (Cembrane) was 0.1 µm and the total filtration area of a module was 0.049 m^2. An intermittent suction of 5 min on and 1 min relaxation cycles were adopted to decrease the cake formation on the membrane. The bioreactor was continuously aerated to keep dissolved oxygen ≥3 mg/L and scour the cake deposited on the membrane. The bioreactor was operated without any temperature control at 27±1.6 ºC. The CMBR operated in our previous study for 205 days (Demir et al., 2020) was dominated by *Acidiphilium cryptum* and *Alicyclobacillus cycloheptanicus*.

In the present study, the Fe^{2+} oxidation performance of CMBR was evaluated in the presence of other heavy metals (Cu, Co, Mn, Zn, and Ni) and As possibly found in AMD (Table 1). Synthetic wastewater was prepared with tap water whose pH value was adjusted to 2.0 using concentrated H_2SO_4. Nutrients and the metals prepared as 100 times concentrated solutions were supplemented to reach desired concentrations provided in Table 1. H_2AsKO_4 was used in the preparation of As(V) stock solution. The synthetic AMD was also supplemented with 250 mg/L TSB as an organic carbon and nutrient source to support biomass growth. When the bioreactor was fed with TSB free media (period 6, Table 2), 22 mg/L KH_2PO_4 was added as a P source for bacterial growth.

In the beginning, the CMBR was fed with metal-free media (period 1, Table 2) to evaluate the Fe^{2+} oxidation performance in the absence of high heavy metal concentrations. Metals at low concentrations were supplemented as nutrients as presented in Table 1. After period 1, metals provided as a separate column in Table 1 were added to the nutrient-supplemented media to simulate AMD.

2.2. Operational Conditions of the Ceramic Membrane Bioreactor

The CMBR was operated under varying operational conditions (Table 2). In the first period (Table 2), the bioreactor was fed with 250 mg/L Fe^{2+} in the absence of metal mixture at an HRT of 24 h. In the 2nd period, the metal mixture was added to the feed and the bioreactor performance was evaluated under varying HRTs and fluxes. In the 3rd and the 4th periods, HRT was decreased to 12 h and 6 h, respectively, keeping the influent Fe^{2+} concentration at 250 mg/L. In the 5th period, feed Fe^{2+} concentration was increased to 750 mg/L to evaluated the bioreactor performance under increasing Fe^{2+} loading. Lastly in the 6th period, TSB was eliminated from the synthetic feed. The Fe^{2+} loading rate in the CMBR was changed between 0.25 and 3.0 g/(L.d) by varying the feed Fe^{2+} or HRT.

At the end of each period, continuous operation of the CMBR was ceased and a concentrated Fe^{2+} solution was directly added to the CMBR. The CMBR was then operated batch-wise under aeration and the reactor was sampled to evaluate the time course variation of Fe^{2+}, ORP, and pH. The batch operation was continued until the ORP value reached the one recorded during the continuous operation, i.e. ORP > 600 mV. In this way, the impacts of operational conditions (Table 2) on the Fe^{2+} oxidation rates were also evaluated under batch cycles of CMBR similar to our previous study (Demir et al., 2020).

Membrane fouling was monitored by the transmembrane pressure (TMP) measurements. The fluxes in the CMBR were changed between 2.55 and 10.2 LMH depending on the HRT and

the numbers of modules (Table 2). When TMP exceeds around 400 mbar, a permeate backwash was provided to scour the cake/gel layer on the membrane. Only one chemical cleaning was applied on day 90 in a 1 M H_2SO_4 solution first and then in a 1% NaOCl solution for 1 day. On day 99, periodic backwash cycles were started to alleviate membrane fouling. The membranes were back-washed with permeate at 30 LMH flux for 1 min durations every three hours of operation.

In period-5, the CMBR content was also sampled for the measurement of specific resistance to filtration (SRF), supernatant filterability (SF), capillary suction time (CST), and viscosity.

2.3. Evaluating the Impact of TSB and Fe^{2+} Concentration in Batch Tests

First of all, a 1 L batch reactor was set up with a 10 mL sludge obtained from the CMBR on day 66 and the batch reactor was fed with initial TSB and Fe^{2+} concentrations of 250 mg/L each. The reactor was fed with the same concentrated solution three cycles to acclimate the biomass to batch operation. Then, three parallel 1 L batch reactors were operated to evaluate the impacts of Fe^{2+} and TSB concentrations on the Fe^{2+} oxidation rate and biomass growth. The initial TSB concentrations in all the parallels were 25 mg/L and the initial pHs were adjusted to around 2.0 using sulfuric acid. All the reactors were seeded with 250 mL sludge obtained from the batch reactor described above. In this way, biomass already acclimated to batch conditions were used. The first batch reactor (BR-1) was operated in the absence of Fe^{2+}, whereas in the second (BR-2) and the third one (BR-3), the initial Fe^{2+} concentrations were 250 mg/L and 2500 mg/L, respectively. After around 45 h operation of the BR-1, 250 mg/L TSB was supplemented to see whether biomass grew in Fe^{2+} free media. The operational conditions of the batch reactors were summarized in Table 3.

2.4. Co-precipitation of Iron and Arsenic as Biogenic Schwertmannite

At the end of periods 2, 5, and 6 (Table 2), CMBR permeate was used for simultaneous Fe^{3+} and As(V) precipitation. For this purpose, 5 N NaOH was added to the CMBR permeate collected in period-2 and the pH was raised to 3.0, 3.5, 4.0, and 4.5 to decide the optimum pH for co-precipitation and/or adsorptive removal of As(V) together with Fe^{3+}. The experiments conducted in period-2 illustrated that both Fe and As removals at pH 3.0 were only partial and, therefore, in the other periods (5 and 6), pH was raised to 3.5 and 4.0 to produce biogenic schwertmannite for selective co-precipitation of Fe and As. In the experiments, pH of 250 mL permeate was adjusted to the target value under around 5 min vigorous mixing. Then, the permeate was left settling for around 30 min in a graduated cylinder. The supernatant was syringe filtered for subsequent metal and As measurements.

2.5. Bacterial Community Analyses

The bacterial community analyses were investigated according to our previous study (Demir et al., 2020). The bacterial cultures of first period was used for the extraction of total DNA (Demir et al., 2020; Nural Yaman et al., 2020). The total DNA with high quality were sent to service (BM Software Consultancy and Lab, System Co Ltd., Ankara, Turkey) for 16S Amplicon Sequencing which was performed by Illumina Miseq Platform (Demir et al., 2020).

The raw data were analyzed by QIIME 2020.2 environment. The quality controls of paired end sequences were done by FASTQC. The command with DADA2 filtered the quality scores in the paired end sequences to correct errors and remove the chimeras. Close reference clustering of OTUs were preferred and aligned against the NCBI database (Nural Yaman et al., 2020). All files were visualized by QIIME2 view toolbar (https://view.qiime2. org/).

2.6. Relative quantification Real Time PCR

Relative quantification is based on the PCR signal received from the target transcript in sampling group. The $2^{-\Delta\Delta CT}$ method is convenient to analyse the changes in community (Livak and Schmittgen, 2001). Relative quantification Real-time PCR using SYBR green I or Taqman Probe was employed with the specific primer sets to determine the gene copy number of different microbial groups (Tajadini et al., 2014).

Designed primer pairs and universal primer pairs for 16S rRNA (Table 4) were used for Relative Quantitative $2^{-\Delta\Delta CT}$ method. All reactions were carried out in ABI 7500 (Thermo Scientific, USA). The total volume of the PCR reaction mix was 20 μL made up of SYBER Green master mix 1x, forward and reverse primer 10 μM and 2 μL template cDNA. For each assay, all samples were run in triplicate. The thermal cycling conditions were 40 cycles of 95 ºC for 15 s and 60 ºC for 60 s, one cycle with an initial 95 ºC denaturation (15 min). The relative expression levels were calculated using the $2^{-\Delta\Delta CT}$ method of (Livak and Schmittgen, 2001).

2.7. Analytical Methods

For the measurements of Fe, COD, MLSS, and MLVSS concentrations Standard Methods (APHA, 2005) were used. In the permeate, COD and Fe^{2+} were measured without further filtration. The colorimetric ortho-phenanthroline method given in Standard Methods (APHA, 2005) was used for Fe^{2+} measurement. TSB concentration was measured as COD and the contribution of Fe^{2+} to the COD was excluded considering theoretical oxygen demand of Fe^{2+} (0.14 mg-O_2/mg-Fe^{2+}) according to R-2.

To measure total Fe, first of all, Fe^{3+} was reduced to Fe^{2+} using ascorbic acid (Jones and Johnson, 2015). Then, Fe^{2+} was measured and expressed as total Fe. Total arsenic (without differentiating As (III) and As(V)) and other metals were measured using Thermo ICAP RQ

ICP-MS at Osmangazi University Central Research Laboratory Application and Research Center (ARUM, Eskişehir, Turkey). ORP WTW Multi 3420 and HACH HQ40d multimeter were used for ORP and pH measurements, respectively.

Fe^{2+} was analyzed only once considering a stable calibration curve, less than 3% error in the measurements and the regular (three times a week) sampling. The heavy metals and arsenic were measured in triplicates.

Specific resistance to filtration (SRF), supernatant filterability (SF), capillary suction time (CST), and viscosity were measured according to Dereli et al. (2014).

3. Results and Discussion

3.1. Performance of Continuously Operated CMBR

In the first period, the performance of Fe^{2+} oxidation was evaluated in the absence of other heavy metals at an HRT of 24 h. Almost complete Fe^{2+} oxidation was obtained with the permeate Fe^{2+} concentration of 1.8±0.1 mg/L. The feed and the permeate ORP values were 372±12 mV and 613±8 mV, respectively (Fig. 1). The COD in the feed and the permeate was 178±28 mg/L and 24±13 mg/L, respectively, corresponding to 87% COD removal.

In the second period (days 20-41), heavy metals (Table 1) were supplemented to investigate their impact on Fe^{2+} oxidation performance while keeping the other operational conditions constant (Table 2). Fe^{2+} oxidation performance was not adversely affected as permeate Fe^{2+} concentration was 1.5±0.5 mg/L, corresponding with >99% oxidation, together with ORP values of 608±8 mV (Fig. 1). The mean influent and permeate COD concentrations were 198±15 mg/L and 45±6 mg/L, respectively, corresponding to 77% COD oxidation.

In the third period (days 41-59), HRT was decreased to 12 h by doubling the feed flow rate keeping all the other operational conditions constant (Table 2). Membrane flux increased from

2.55 L/(m^2.h) (LMH) to 5.1 LMH. Although the HRT in the bioreactor was decreased, the permeate Fe^{2+} concentration averaged 1.6±0.3 mg/L, corresponding to >99% oxidation efficiency. The average ORP value increased from 379 mV in the influent to around 608 mV in the permeate. The mean influent and permeate COD concentrations were 193±4 and 39±2 mg/L, respectively, corresponding to around 80% oxidation performance.

In the fourth period (days 59-83), the feed flow rate was increased to an HRT of 6 h (Table 2). Increasing the flux to 10.2 LMH resulted in significant membrane fouling (to be discussed later) as TMP increased to 800-900 mbar although the membrane was back-washed regularly once every two days. In this period, the feed overflew three times. One more membrane was added to the bioreactor on day 66 to decrease the flux back to 5.1 LMH, after which TMP did not exceed 500 mbar until day 81. Although the HRT in the CMBR was decreased substantially, Fe^{2+} concentration at the permeate averaged 2.8±2.1 mg/L, corresponding to around 99% oxidation efficiency. The average ORP value at the influent was 368 mV and increased to around 567 mV at the permeate. In this period, the average feed and permeate COD concentrations were 191±5 and 43±5 mg/L (77% oxidation), respectively.

In the fifth period (days 83-105), the influent Fe^{2+} was increased to 750 mg/L keeping all the other operational conditions constant (Table 2). The Fe^{2+} concentration at the permeate of the bioreactor increased to 20±7 mg/L corresponding to >97% oxidation efficiency. The average ORP increased from the influent 353 mV to 577 mV in the permeate. The influent and permeate COD concentrations were 200±6 and 49±5 mg/L, respectively, corresponding to 76% oxidation efficiency.

In the sixth period (days 105-131), TSB was eliminated from the feed (Table 2) to evaluate the bioreactor performance in the absence of an external organic matter for 26 days of operation. Fe^{2+} concentration in the permeate was 13±0.2 mg/L corresponding to 98% oxidation efficiency. The ORP increased from 352 mV in the influent to 645 mV in the

permeate. High Fe^{2+} oxidation performances (97-99%) were similar to those reported in our previous study (Demir et al., 2020).

Permeate Fe^{2+} concentrations were in line with the ORP results. Fe precipitation (Fig. 2) within the bioreactor was not observed, which may be due to relatively low pH (2.1±0.06) and low Fe, Na^+, K^+ and, NH_4^+ concentrations and, hence, jarosite formation was negligible similar to our previous study (Demir et al., 2020).

Influent and permeate pHs were 2.0±0.02 and 2.1±0.06, respectively, throughout the study. However, pH was slightly higher in the permeate during periods 5-6 (2.16±0.02) compared to periods 1-4 (2.07±0.05) (Fig. 3), which may be due to higher H^+ ion consumption during Fe^{2+} oxidation according to R-2. The suspended (SS) and volatile suspended solid (VSS) concentrations in the CMBR showed an increasing trend (Fig. 3) as sludge was not wasted from the bioreactor except for sampling. Hence, SRT may be considered as infinite. The VSS was 4170±990 mg/L in period 5 and 4370±144 mg/L in period 6. Thus, the biomass growth during the last period was rather slow.

The influent and the permeate COD concentrations averaged 193±12 mg/L and 40±10 mg/L, respectively, between periods 1 and 5 (data not shown).

During the operation of the CMBR, no removal of metals was detected (data not shown) due to relatively low pH and no or undetectable formation of Fe containing precipitates, such as jarosite, to which metals or metalloids can be adsorbed. After biological oxidation of Fe^{2+} according to R-2, jarosite formation may be described with the following reaction (Bigham et al., 2010).

$$3Fe^{3+} + M^+ + 2SO_4^{2-} + 6H_2O \rightarrow MFe_3(SO_4)_2(OH)_6 + 6H^+ \quad \text{(R-8)}$$

Where M refers to monovalent ions, such as K^+, Na^+, NH_4^+, and H_3O^+.

Daoud and Karamanev (2006) studied the optimum temperature and pH at which jarosite formation was minimal and Fe^{2+} oxidation by *Acidithiobacillus ferrooxidans* was at high rates. They reported a high Fe^{2+} oxidation rate and insignificant jarosite formation at room temperature (22 ^{o}C) and pH from 1.6 to 2.0. The jarosite formation, hence, mainly depended on pH, temperature, and the concentrations of Fe and monovalent ions, i.e. K^{+}, Na^{+}, NH_4^{+}, and H_3O^{+} (R-8) (Bigham et al., 2010). In our study, total feed and permeate iron concentrations were nearly the same (Fig. 2), and jarosite formation and associated arsenic removal remained negligible throughout the study.

3.2. Filtration performance in the CMBR

During the operation of the CMBR at 2.55 LMH, no significant membrane fouling (monitored as TMP) was detected (Fig. 4). Between days 41 and 59, flux was increased to 5.1 LMH with no significant fouling. Then, the flux increased to 10.2 LMH with decreasing the HRT to 6 h when the CMBR was operated with the one membrane module. The TMP several times exceeded the 800 mbar although the membrane was physically cleaned once every two days by backwashing with the permeate. After day 66, one more module was integrated and the flux was decreased back to 5.1 LMH to alleviate the membrane fouling. The membrane fouling decreased significantly and after operation of around 14 days, TMP increased to around 500 mbar on day 81 at which a backwash was applied to clean the membrane. After increasing the feed Fe^{2+} to 750 mg/L on day 83, the membrane fouling increased. This may be due to pore blocking by small amount of Fe-containing precipitates, e.g. jarosite at pH of 2.0, although not detected by total Fe analyses in the feed and permeate. Physical membrane cleanings were applied almost every two days and on day 90 both membrane modules were chemically cleaned. However, TMP values still increased to high values within two days, which resulted three times in CMBR overflow.

On day 99, periodic backwash of the membranes with the permeate (1 min at 30 LMH flux) every three hours of operation was applied to alleviate the membrane fouling. Although regular backwashing decreased the membrane fouling, more studies are required to optimize the membrane filtration performance.

Also, the filterability of the sludge in period 5 on two different days, i.e. 97 and 101, were assessed. The SRF, SF, CST, and viscosity were $1.1\pm0.5x10^{15}$ m/kg, 0.48±0.17 mL/min, 72.0±4.0 s, and 2.14±0.12 cP, respectively. The filterability depends on many factors including the operational conditions, especially SRT (Pollice et al., 2008) and the wastewater being treated. In our study, the mixed liquor is composed of high concentrations of metals at pH of ~2, which may make the comparison with the results obtained with municipal or many other industrial wastewaters irrelevant. For example, Pollice et al. (2008) reported the SRF values being in the range of 10^{10}-10^{12} m/kg for the sludge samples obtained from MBR treating real municipal wastewater.

CST may be used as an easily measurable parameter to obtain insight into sludge filterability in an MBR (Wang et al., 2006) and/or early warning for the membrane cleaning (Pollice et al., 2008). A high value of CST indicates poor filterability of the sludge. Gabarrón et al. (2013) reported full-scale MBR treatment data for municipal wastewater and reported a CST value of 62±10 s.

3.3. Iron Oxidation Rates in Batch Operational Cycles of CMBR

The Fe^{2+} oxidation rates under varying conditions (Table 2) were determined by operating the CMBR in batch mode. The variations of Fe^{2+} and ORP values for batch operation of CMBR after each period were as illustrated in Fig. 5. The Fe^{2+} oxidation was completed within around 250 min in the first period, i.e. in the absence of metal mixture, and the Fe^{2+} oxidation rate was calculated as 0.97 mg Fe^{2+}/(L.min). When the medium was supplemented with a

mixed metal cocktail, the Fe^{2+} oxidation rate remained almost similar at 0.98 mg Fe^{2+}/(L.min). Batch experiments at the end of periods 3 and 4 were also conducted to determine the impact of HRT on the Fe^{2+} oxidation rates of biomass. The Fe^{2+} oxidation rates were calculated as 1.3 and 5.16 mg Fe^{2+}/(L.min) in periods 3 and 4 corresponding to HRTs of 12 and 6 h in CMBR, respectively. Hence, decreasing the HRT (or rather increasing the loading rate) significantly increased the Fe^{2+} oxidation rate of biomass.

In period 5, increasing the feed Fe^{2+} concentration to 750 mg/L significantly increased the Fe^{2+} oxidation rate to 21.75 mg Fe^{2+}/(L.min). Hence, the Fe^{2+} oxidation rate depends on its loading rate to the bioreactor.

In the last period, CMBR was operated with organic matter free media and batch test showed that the Fe^{2+} oxidation rate decreased significantly to 10.68 mg Fe^{2+}/(L.min). The final Fe^{2+} concentration was around 15 mg/L, which was similar to the one observed in the period-5 (17 mg/L). The ORP data measured during the batch operations also illustrated the rate of Fe^{2+} oxidation as the values decreased to 460-470 mV after Fe^{2+} addition and it increased to 670-680 mV at the end of the batch operations. The increase rate of ORP completely depended on the Fe^{2+} oxidation rate (Fig. 5).

The specific Fe^{2+} oxidation rates were provided in Fig. 6. The supplementation of metal mixture in period 2 decreased the specific Fe^{2+} oxidation rate from 0.76 to 0.47 mg-Fe^{2+}/(g-VSS.min), hence metal mixture may have some inhibitory effect on specific Fe^{2+} oxidation. Observing similar Fe^{2+} oxidation rate as mg-Fe^{2+}/(L.min), which was discussed above, but lower specific Fe^{2+} oxidation rate as mg-Fe^{2+}/(g-VSS.min) was due to the higher biomass concentration in period 2 (2.07 g/L) compared to period 1 (1.27 g/L).

Increasing the Fe^{2+} loading rate to the CMBR significantly increased the specific Fe oxidation rate reaching the capacity of 6.3 mg-Fe^{2+}/(g-VSS.min), in period 5. Removal of the TSB from

the feed decreased the specific Fe^{2+} oxidation rate to around 2.36 mg-Fe^{2+}/(g-VSS.min). Hence, the elimination of TSB significantly decreased the specific Fe^{2+} oxidation rate in long-term operation.

In our previous study (Demir et al., 2020), the Fe^{2+} oxidation rate followed Monod Equation with a half-saturation constant of 549 mg/L. Hence, an increasing specific Fe^{2+} oxidation rate may be expected from the increasing feed Fe^{2+} concentration from 250 mg/L to 750 mg/L. The biomass used in the kinetics assays in our previous study (Demir et al., 2020) was obtained from the CMBR fed with around 1400 mg/L Fe^{2+} at an HRT of 48 h. Hence, the obtained specific Fe^{2+} oxidation rates are valid only under the studied operating conditions.

3.4. Evaluating the Impact of TSB and Fe^{2+} Concentrations in Batch Assays

Biomass growth in the absence of Fe^{2+} (BR-1) and at different initial Fe^{2+} concentrations (BR-2 and BR-3) was studied in batch assays (Table 3). In the presence of 25 mg/L TSB, no or negligible biomass growth (as OD_{620}) occurred in the absence (BR-1) and presence of 250 mg/L Fe^{2+} (BR-2). When 250 mg/L TSB was supplemented to the BR-1, OD_{620} increased substantially (Fig. 7). The initial biomass concentration in all the batches was around 70 mg/L and the final biomass concentrations in BR-1 for 25 mg/L and 250 mg/L TSB were as illustrated in Fig. 7. Hence, biomass growth occurred even in the absence of Fe^{2+}, demonstrating that the mixed culture uses TSB as a carbon and energy source.

According to Jones and Johnson (2016), free energy generation from Fe^{2+} oxidation is very small ($\Delta G^0 = -47$ kJ/mol) compared to glucose ($\Delta G^0 = -2880$ kJ/mol). Hence, in order to elucidate whether biomass obtains energy from Fe^{2+} oxidation, its concentration was kept much higher compared to TSB. Considering the study of Johnson et al. (1992), TSB concentration was kept at 25 mg/L in BR-2 and BR-3, whereas Fe^{2+} concentration was kept at significantly high levels, i.e., 250 mg/L in BR-2 and 2500 mg/L in BR-3. Fe^{2+} oxidation was

completed within around 45 h and 100 h in the BR-2 and BR-3, respectively (data not shown). The initial biomass concentration in all the batches was around 70 mg/L and final VSS concentrations in BR-2 (25 mg/L TSB and 250 mg/L Fe^{2+}) and BR-3 (25 mg/L TSB and 2500 mg/L Fe^{2+}) were around 74 mg/L and 93 mg/L, respectively (Fig. 7). Hence, slightly higher amount of biomass growth was observed when the media was supplemented with significantly higher initial Fe^{2+} concentration.

3.5. 16S Amplicon Sequencing

Microbial community was determined by 16S Amplicon Sequencing for the sample taken from the bioreactor during the first period (Table 2), i.e., in the absence of metal cocktail in the feed. The bioinformatic analysis was performed by 100% identity in closed reference. At the end of the analysis, *Alicyclobacillus tolerans* and *Acidiphilium cryptum* were identified at species level. The percentages of these bacteria were 48% and 45%, respectively. *Alicyclobacillus* spp. have been observed in various mixed bioleaching cultures obtained from mine sites (Halinen et al., 2012; Kaksonen et al., 2016; Yahya et al., 2008). *Alicyclobacillus tolerans*, which is formerly classified in the genus *Sulfobacillus*, is aerobic, Gram-positive, spore-forming rod and grows in the presence of organic compounds and Fe^{2+} (Kaksonen et al., 2016; Karavaiko et al., 2005). *Alicyclobacillus tolerans* has high tolerance to the changes in temperature and pH as it grows in a temperature and pH ranges of <20-55 ºC (optimum 37-42 ºC) and 1.5-5.0 (optimum 2.5-2.7), respectively (Karavaiko et al., 2005). *Acidiphilium cryptum* is an obligate heterotroph and iron reducing microorganism that can be found in AMD (Falagán and Johnson, 2018; González et al., 2018).

3.6. Relative quantification Real Time PCR

The DNAs extracted from the sludge samples taken from the CMBR during the four different periods (periods 1,3,5 and 6 in Table 2) were analysed with the specific primers. The relative quantifications of the *Alicyclobacillus tolerans* and *Acidiphilium cryptum* in the samples were

calculated and the impacts of the operational conditions (Table 2) on the relative variations of the species were determined. The first operational period in which metal cocktails were not supplemented to the feed was used as a baseline and the relative contribution of the species identified by amplicon sequencing in other periods were comparatively evaluated.

As the first period was accepted to be the baseline period, the relative quantity of both species in period-1 was accepted as 1.0 and the relative quantity of each specie in other periods was determined. In the third period, the relative quantities of *Alicyclobacillus tolerans* and *Acidiphilium cryptum* increased to 27.4 and 1.6, respectively, which should be due to increased Fe^{2+} loadings from 0.25 g/(L.d) in period-1 to 0.5 g/(L.d) in period-3. With a 12-fold increase in the Fe^{2+} loading in period-5, relative quantities of *Alicyclobacillus tolerans* and *Acidiphilium cryptum* increased to 42.0 and 77.0, respectively (Table 5). However, in the last period the relative quantities of *Alicyclobacillus tolerans* and *Acidiphilium cryptum* decreased to 6.47 and 0.006, respectively, which should be due to the elimination of organic matter, TSB, from the feeding media (Table 5). Almost total disappearance of the *Acidiphilium cryptum* is an expected result as it is an obligate heterotroph (Falagán and Johnson, 2018) and could not be sustained in period-6 due to feeding of the bioreactor with an organic matter free medium (Table 2). *Alicyclobacillus tolerans* is a facultative chemo-organoheterotroph and mixotroph strain, but shows better growth under mixotrophic growth conditions rather than on organics alone (da Costa et al., 2015; Karavaiko et al., 2005). Holanda and Johnson (2020) reported that *Alicyclobacillus tolerans* can grow both heterotrophically and autotrophically on Fe^{2+}. Hence, in period 6, in which the organic matter was excluded from the feed, *Alicyclobacillus tolerans* was sustained but with a decreased relative quantity compared to the previous periods.

3.7. Co-precipitation of Iron and Arsenic as Biogenic Schwertmannite

Co-precipitation of As and Fe, as schwertmannite, is favored by pH ranging from 2.8 to 4.5 (Wang et al., 2006). The schwertmannite formation is represented by the following reaction (Hedrich and Johnson, 2012).

$$8Fe^{3+} + SO_4^{2-} + 14H_2O \rightarrow Fe_8O_8(OH)_6(SO_4) + 22H^+ \quad \text{(R-9)}$$

In period 2 (the permeate contained 250 mg/L Fe and 25 mg/L As and Fe/As ratio of 10), the pH effects on the co-precipitation performance was investigated. The pH was adjusted to 3.0, 3.5, 4.0, and 4.5 in parallel batch tests, and the soluble Fe and As concentrations were as given in Fig. 8. The initial As concentration was around 27 mg/L and decreased to 10.7, 0.82, 0.5 and 0.25 mg/L at pH of 3.0, 3.5, 4.0 and 4.5, respectively. Hence, As removal efficiency was only 60% at pH 3.0 and increased to 97% at pH 3.5. Further increasing the pH increased the removal performance even to 99% at pH 4.5. The pH 3.5, however, may be considered optimal. The total Fe concentration in the permeate (period 2) was around 260 mg/L and it decreased to 181, 2.52, 0.34, and 1.21 mg/L at pH of 3.0, 3.5, 4.0, and 4.5, respectively. Hence, at pH 3.5 quite high Fe removal efficiency was also attained. At pH 3.0 only 30% Fe precipitated which may have resulted in partial As removal at pH 3.0.

In periods 5 and 6, the similar experiment was also conducted at pH 3.5 and 4.0 and at initial Fe/As ratio of 30. In both periods, Fe precipitation were similar with the total Fe concentrations of 3.7 mg/L at pH 3.5 in both periods. The total Fe concentrations decreased to around 1.44 and 0.93 at pH 4.0 in periods 5 and 6, respectively. As in the permeate decreased to around 0.5 and 0.09 mg/L at pH 3.5 in periods 5 and 6, respectively. When the pH was increased to 4.0, the permeate As concentrations decreased to 0.37 and 0.07 mg/L in respective order (Fig. 8). Hence, co-precipitation of Fe and As with biogenic schwertmannite production at pH 3.5 results in 98-99% removals of Fe and As. Similarly, Ahoranta et al.

(2016) reported As removal at pH 3.0 as high as 99.5%, corresponding to a total As concentration of 0.03 mg/L, in the effluent of settling tank integrated to a FBR. The higher removal at pH 3.0 in the study of Ahoranta et al. (2016), compared to the present study, was likely due to much higher Fe^{2+} concentration (5 g/L) used.

The other metals remained in solution during the schwertmannite precipitation as expected due to relatively low pH (data not shown). Hence, sulfidogenic anaerobic processes may be used as down-stream process to recover valuable metals (Bayrakdar et al., 2009) after schwertmannite precipitation.

4. Conclusions

The CMBR performance for the Fe^{2+} oxidation in a synthetic AMD was revealed at varying Fe^{2+} loadings (0.25-3.0 g/(L.d)), and in the presence and absence of TSB with the following conclusions:

- 98-99% of iron oxidation is obtained in CMBR.
- The metal mixture supplementation decreases the specific Fe^{2+} oxidation rate from 0.76 to 0.47 mg Fe^{2+}/(g-VSS.min).
- The specific Fe^{2+} oxidation rate up to 6.3 mg Fe^{2+}/(g-VSS.min) can be obtained whilst the removal of TSB from the feed decreases the rate by 62% to 2.4 mg Fe^{2+}/(g-VSS.min).
- 99% selective co-precipitation of As and Fe associated with schwertmannite precipitation is triggered by controlling pH to 3.5-4.0 with NaOH.
- Sustainable membrane filtration of up to 5.0 LMH is achieved by regular backwash without long term chemical cleaning.
- *Alicyclobacillus tolerans* and *Acidiphilium cryptum* dominate the mixed culture.

- *Acidiphilium cryptum*, an obligate heterotroph, is almost eliminated from the mixed culture when the bioreactor is fed with organic free media.

Acknowledgement

This work was supported by the Research Fund of Istanbul Medeniyet University. Project Number: F-GAP-2019-1487.

References

Ahoranta, S., Hulkkonen, H., Salminen, T., Kuula, P., Puhakka, J.A., Lakaniemi, A.M., 2020. Formation and use of biogenic jarosite carrier for high-rate iron oxidising biofilms. Res. Microbiol. 171, 243–251. https://doi.org/10.1016/j.resmic.2020.06.004

Ahoranta, S.H., Kokko, M.E., Papirio, S., Özkaya, B., Puhakka, J.A., 2016. Arsenic removal from acidic solutions with biogenic ferric precipitates. J. Hazard. Mater. 306, 124–132. https://doi.org/10.1016/j.jhazmat.2015.12.012

APHA, 2005. Standard Methods for the Examination of Water and Wastewater. Washington DC, USA.

Aytar, P., Kay, C.M., Mutlu, M.B., Çabuk, A., Johnson, D.B., 2015. Diversity of acidophilic prokaryotes at two acid mine drainage sites in Turkey. Environ. Sci. Pollut. Res. 22, 5995–6003. https://doi.org/10.1007/s11356-014-3789-4

Bayrakdar, A., Sahinkaya, E., Gungor, M., Uyanik, S., Atasoy, A.D., 2009. Performance of sulfidogenic anaerobic baffled reactor (ABR) treating acidic and zinc-containing wastewater. Bioresour. Technol. 100, 4354–4360. https://doi.org/10.1016/j.biortech.2009.04.028

Bigham, J.M., Jones, F.S., Özkaya, B., Sahinkaya, E., Puhakka, J.A., Tuovinen, O.H., 2010. Characterization of jarosites produced by chemical synthesis over a temperature gradient

from 2 to 40 °C. Int. J. Miner. Process. 94, 121–128. https://doi.org/10.1016/j.minpro.2010.01.005

Bissen, M., Frimmel, F.H., Ag, C., 2003. Arsenic - A review. Part I: Occurrence, toxicity, speciation, mobility. Acta Hydrochim. Hydrobiol. 31, 9–18. https://doi.org/10.1002/aheh.200390025

Blodau, C., 2006. A review of acidity generation and consumption in acidic coal mine lakes and their watersheds. Sci. Total Environ. 369, 307–332. https://doi.org/10.1016/j.scitotenv.2006.05.004

Casiot, C., Morin, G., Juillot, F., Bruneel, O., Personné, J.C., Leblanc, M., Duquesne, K., Bonnefoy, V., Elbaz-Poulichet, F., 2003. Bacterial immobilization and oxidation of arsenic in acid mine drainage (Carnoulès creek, France). Water Res. 37, 2929–2936. https://doi.org/10.1016/S0043-1354(03)00080-0

da Costa, M.S., Rainey, F.A., Albuquerque, L., 2015. Alicyclobacillus. Bergey's Man. Syst. Archaea Bact. 1–18. https://doi.org/10.1002/9781118960608.gbm00526

Daoud, J., Karamanev, D., 2006. Formation of jarosite during Fe2+ oxidation by Acidithiobacillus ferrooxidans. Miner. Eng. 19, 960–967. https://doi.org/10.1016/j.mineng.2005.10.024

Demir, E.K., Yaman, B.N., Çelik, P.A., Sahinkaya, E., 2020. Iron oxidation in a ceramic membrane bioreactor using acidophilic bacteria isolated from an acid mine drainage. J. Water Process Eng. 38, 101610. https://doi.org/10.1016/j.jwpe.2020.101610

Dereli, R.K., Grelot, A., Heffernan, B., van der Zee, F.P., van Lier, J.B., 2014. Implications of changes in solids retention time on long term evolution of sludge filterability in anaerobic membrane bioreactors treating high strength industrial wastewater. Water Res.

59, 11–22. https://doi.org/10.1016/j.watres.2014.03.073

Falagán, C., Johnson, D.B., 2018. The significance of pH in dictating the relative toxicities of chloride and copper to acidophilic bacteria. Res. Microbiol. 169, 552–557. https://doi.org/10.1016/j.resmic.2018.07.004

Gabarrón, S., Gómez, M., Monclús, H., Rodríguez-Roda, I., Comas, J., 2013. Ragging phenomenon characterisation and impact in a full-scale MBR. Water Sci. Technol. 67, 810–816. https://doi.org/10.2166/wst.2012.633

González, E., Rodríguez, J.M., Muñoz, J.Á., Blázquez, M.L., Ballester, A., González, F., 2018. The contribution of Acidiphilium cryptum to the dissolution of low-grade manganese ores. Hydrometallurgy 175, 312–318. https://doi.org/10.1016/j.hydromet.2017.12.008

Halinen, A.K., Beecroft, N.J., Määttä, K., Nurmi, P., Laukkanen, K., Kaksonen, A.H., Riekkola-Vanhanen, M., Puhakka, J.A., 2012. Microbial community dynamics during a demonstration-scale bioheap leaching operation. Hydrometallurgy 125–126, 34–41. https://doi.org/10.1016/j.hydromet.2012.05.001

Hedrich, S., Johnson, D.B., 2012. A modular continuous flow reactor system for the selective bio-oxidation of iron and precipitation of schwertmannite from mine-impacted waters. Bioresour. Technol. 106, 44–49. https://doi.org/10.1016/j.biortech.2011.11.130

Holanda, R., Johnson, D.B., 2020. Isolation and characterization of a novel acidophilic zero-valent sulfur- and ferric iron-respiring Firmicute. Res. Microbiol. 171, 215–221. https://doi.org/10.1016/j.resmic.2020.07.003

Huang, L., Lee, D.J., 2015. Membrane bioreactor: A mini review on recent R&D works. Bioresour. Technol. 194, 383–388. https://doi.org/10.1016/j.biortech.2015.07.013

Johnson, D.B., Ghauri, M.A., Said, M.F., 1992. Isolation and characterization of an acidophilic, heterotrophic bacterium capable of oxidizing ferrous iron. Appl. Environ. Microbiol. 58, 1423–1428.

Johnson, D.B., Hallberg, K.B., 2005. Acid mine drainage remediation options: A review. Sci. Total Environ. 338, 3–14. https://doi.org/10.1016/j.scitotenv.2004.09.002

Jones, R.M., Johnson, D.B., 2016. Iron Kinetics and Evolution of Microbial Populations in Low-pH, Ferrous Iron-Oxidizing Bioreactors. Environ. Sci. Technol. 50, 8239–8245. https://doi.org/10.1021/acs.est.6b02141

Jones, R.M., Johnson, D.B., 2015. Acidithrix ferrooxidans gen. nov., sp. nov.; a filamentous and obligately heterotrophic, acidophilic member of the Actinobacteria that catalyzes dissimilatory oxido-reduction of iron. Res. Microbiol. 166, 111–120. https://doi.org/10.1016/j.resmic.2015.01.003

Kaksonen, A.H., Särkijärvi, S., Puhakka, J.A., Peuraniemi, E., Junnikkala, S., Tuovinen, O.H., 2016. Chemical and bacterial leaching of metals from a smelter slag in acid solutions. Hydrometallurgy 159, 46–53. https://doi.org/10.1016/j.hydromet.2015.10.032

Karavaiko, G.I., Bogdanova, T.I., Tourova, T.P., Kondrat'eva, T.F., Tsaplina, I.A., Egorova, M.A., Krasil'nikova, E.N., Zakharchuk, L.M., 2005. Reclassification of "Sulfobacillus thermosulfidooxidans subsp. thermotolerans" strain K1 as Alicyclobacillus tolerans sp. nov. and Sulfobacillus disulfidooxidans Dufresne et al. 1996 as Alicyclobacillus disulfidooxidans comb. nov., and emended description. Int. J. Syst. Evol. Microbiol. 55, 941–947. https://doi.org/10.1099/ijs.0.63300-0

Kefeni, K.K., Msagati, T.A.M., Mamba, B.B., 2017. Acid mine drainage: Prevention, treatment options, and resource recovery: A review. J. Clean. Prod. 151, 475–493. https://doi.org/10.1016/j.jclepro.2017.03.082

Livak, K.J., Schmittgen, T.D., 2001. Analysis of relative gene expression data using real-time quantitative PCR and the 2-ΔΔCT method. Methods 25, 402–408. https://doi.org/10.1006/meth.2001.1262

Natarajan, K.A., 2008. Microbial aspects of acid mine drainage and its bioremediation. Trans. Nonferrous Met. Soc. China 18, 1352–1360. https://doi.org/10.1016/S1003-6326(09)60008-X

Nural Yaman, B., Aytar Çelik, P., Mutlu, M.B., Çabuk, A., 2020. A Combinational Analysis of Acidophilic Bacterial Diversity of an Iron-Rich Environment. Geomicrobiol. J. 37, 877–889. https://doi.org/10.1080/01490451.2020.1795320

Ozkaya, B., Sahinkaya, E., Nurmi, P., Kaksonen, A.H., Puhakka, J.A., 2007. Iron oxidation and precipitation in a simulated heap leaching solution in a Leptospirillum ferriphilum dominated biofilm reactor. Hydrometallurgy 88, 67–74. https://doi.org/10.1016/j.hydromet.2007.02.009

Özkaya, B., Sahinkaya, E., Nurmi, P., Kaksonen, A.H., Puhakka, J.A., 2007. Kinetics of iron oxidation by Leptospirillum ferriphilum dominated culture at pH below one. Biotechnol. Bioeng. 97, 1121–1127. https://doi.org/10.1002/bit.21313

Park, D., Lee, D.S., Park, J.M., 2005. Continuous biological ferrous iron oxidation in a submerged membrane bioreactor. Water Sci. Technol. 51, 59–68.

Pollice, A., Laera, G., Saturno, D., Giordano, C., 2008. Effects of sludge retention time on the performance of a membrane bioreactor treating municipal sewage. J. Memb. Sci. 317, 65–70. https://doi.org/10.1016/j.memsci.2007.08.051

Rowe, O.F., Johnson, D.B., 2008. Comparison of ferric iron generation by different species of acidophilic bacteria immobilized in packed-bed reactors. Syst. Appl. Microbiol. 31, 68–

77. https://doi.org/10.1016/j.syapm.2007.09.001

Sandström, A., Mattsson, E., 2001. Bacterial ferrous iron oxidation of acid mine drainage as pre-treatment for subsequent metal recovery. Int. J. Miner. Process. 62, 309–320. https://doi.org/10.1016/S0301-7516(00)00062-4

Tajadini, M., Panjehpour, M., Javanmard, S.H., 2014. Comparison of SYBR Green and TaqMan methods in quantitative real-time polymerase chain reaction analysis of four adenosine receptor subtypes. Adv. Biomed. Res. 3:85. https://doi.org/10.4103/2277-9175.127998

Wakeman, K.D., Honkavirta, P., Puhakka, J.A., 2011. Bioleaching of flotation by-products of talc production permits the separation of nickel and cobalt from iron and arsenic. Process Biochem. 46, 1589–1598. https://doi.org/10.1016/j.procbio.2011.04.016

Wang, H., Bigham, J.M., Tuovinen, O.H., 2006. Formation of schwertmannite and its transformation to jarosite in the presence of acidophilic iron-oxidizing microorganisms. Mater. Sci. Eng. C 26, 588–592. https://doi.org/10.1016/j.msec.2005.04.009

Wang, Z., Wu, Z., Yu, G., Liu, J., Zhou, Z., 2006. Relationship between sludge characteristics and membrane flux determination in submerged membrane bioreactors. J. Memb. Sci. 284, 87–94. https://doi.org/10.1016/j.memsci.2006.07.006

Yahya, A., Hallberg, K.B., Johnson, D.B., 2008. Iron and carbon metabolism by a mineral-oxidizing Alicyclobacillus-like bacterium. Arch. Microbiol. 189, 305–312. https://doi.org/10.1007/s00203-007-0319-5

List of Tables

Table 1. Simulated AMD composition (pH =2)

Nutrients	**mg/L**	**Metals**	**mg/L**
Fe^{2+}	250 or 750	$CuSO_4.5H_2O$	50 as Cu
$(NH_4)_2SO_4$	1250	$CoCl_2.6H_2O$	10 as Co
$MgSO_4.7H_2O$	500	$MnSO_4.H_2O$	10 as Mn
TSB*	250	$ZnSO_4.7H_2O$	50 as Zn
$ZnSO_4.7H_2O$	10	$NiSO_4.6H_2O$	50 as Ni
$CuSO_4.5H_2O$	1	H_2AsKO_4	25 as As(V)
$CoCl_2.6H_2O$	1		
$NiSO_4.6H_2O$	1		
$MnSO_4.H_2O$	0.8		
H_3BO_3	0.6		

*When the CMBR was fed with TSB free media (period 6, Table 2), around 22 mg/L KH_2PO_4 was supplemented as a P source.

Table 2. Operational periods of the Ceramic MBR

Period	Day	HRT	Fe^{2+} (mg/L)	Fe^{2+} loading (g/L.d)	Flux* (LMH)	Metals Presence
1	0-20	24	250	0.25	2.55	Absent
2	20-41	24	250	0.25	2.55	Table 1
3	41-59	12	250	0.5	5.1	Table 1
4	59-83	6	250	1.0	10.2-5.1	Table 1
5	83-105	6	750	3.0	5.1	Table 1
6**	105-131	6	750	3.0	5.1	Table 1

*One membrane module was used until day 66, then two modules were used.
**The bioreactor was fed with TSB free media.

Table 3. Operational conditions of batch assays

Batch No	TSB (mg/L)	Fe^{2+} (mg/L)	Seed amount (mL)
BR-1	25*	-	250
BR-2	25	250	250
BR-3	25	2500	250

*After around 45 h operation, 250 mg/L TSB was supplemented to see whether biomass grew in Fe^{2+} free media.

Table 4. Primer pairs used in Relative Quantification Real Time PCR

Housekeeping Gene (16S rRNA)	**Forward**	**CGCTAGTAATCGTGGATCAGAATG**
	Reverse	TGTGACGGGCGGTGTGTA
Alicyclobacillus tolerans	Forward	AGGAGAGGGAATGCTCTTTG
	Reverse	GTTGAGCCCTGGMCTTTC
Acidiphilium cryptum	Forward	GGTGGGCACTCTGAAGGAAC
	Reverse	ATCAGCTCGGTGTCACCAC

Table 5: The Replicate Data where target and reference are amplified

Period	Target Name	RQ	C_T	C_T Mean	ΔC_T Mean	$\Delta\Delta C_T$
1	Reference		12.978	12.978		
	Alicyclobacillus tolerans	1	31.927	31.927	18.949	0
	Acidiphilium cryptum	1	19.550	19.550	6.572	0
3	Reference		21.281	21.281		
	Alicyclobacillus tolerans	27.417	35.453	35.453	14.172	-4.777
	Acidiphilium cryptum	1.638	27.140	27.140	5.859	-0.712
5	Reference		20.519	20.519		
	Alicyclobacillus tolerans	41.980	34.077	34.077	13.558	-5.392
	Acidiphilium cryptum	77.035	20.825	20.825	0.305	-6.267
6	Reference		16.602	16.602		
	Alicyclobacillus tolerans	6.470	32.857	32.857	16.255	-2.694
	Acidiphilium cryptum	0.006	30.540	30.540	13.939	7.366

FIGURES

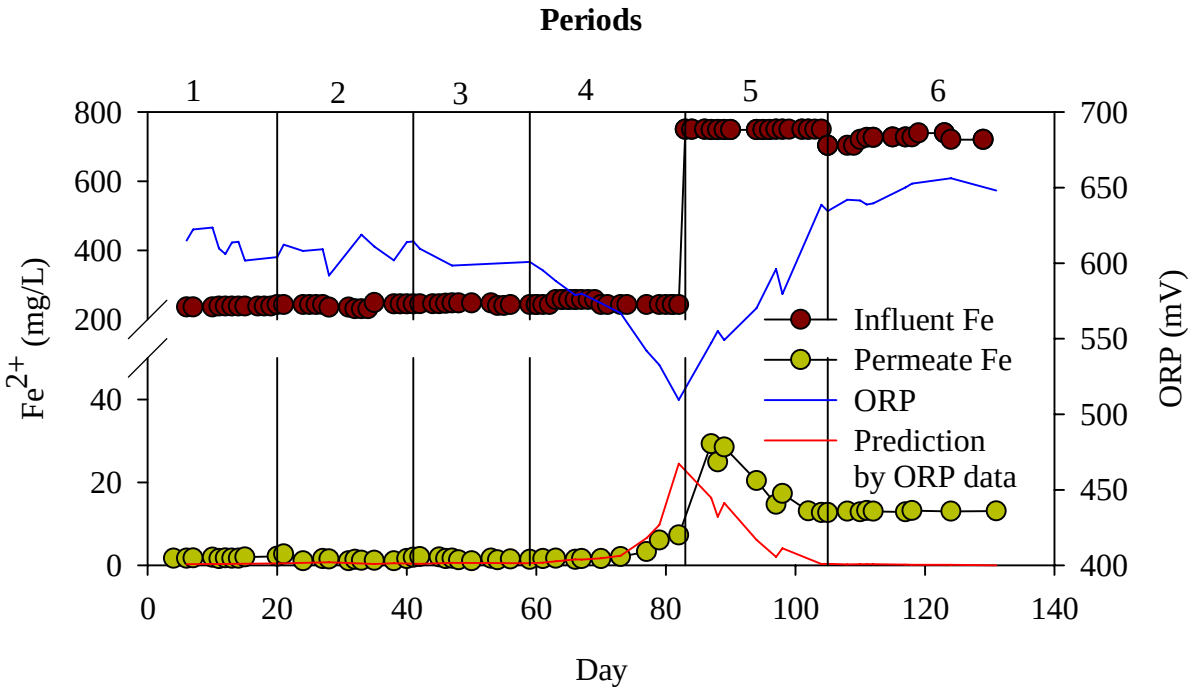

Fig. 1. Iron oxidation performance and ORP under varying operational conditions in the CMBR (Table 2)

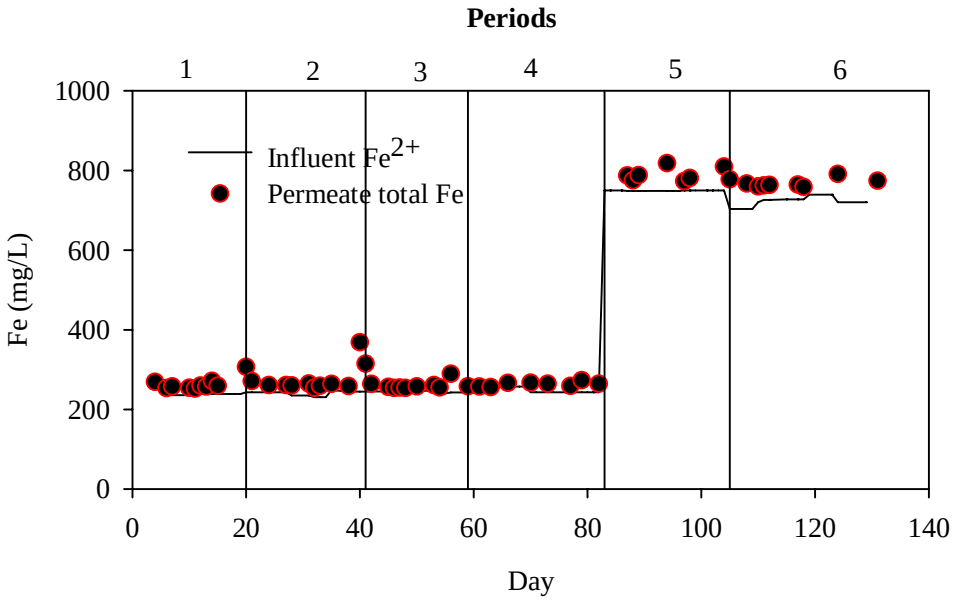

Fig. 2. Total Fe in the influent and permeate of the CMBR

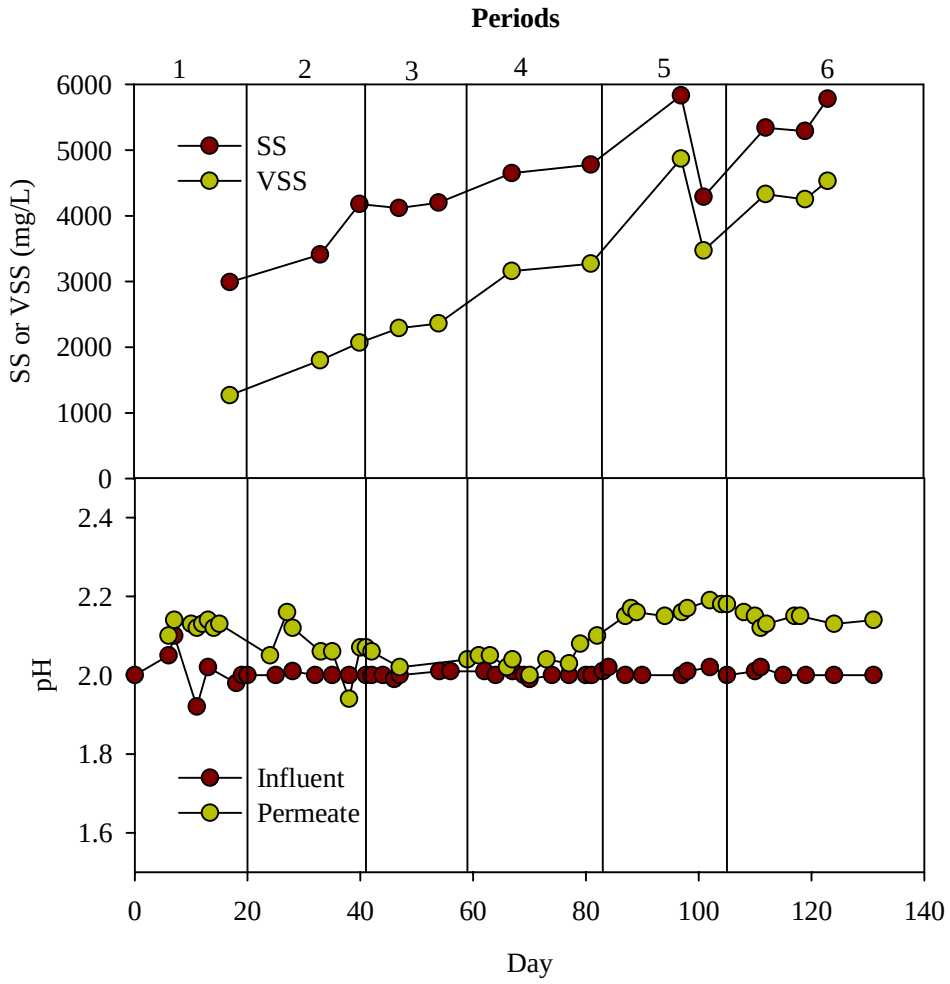

Fig. 3. SS and VSS concentrations together with pH variations in the CMBR

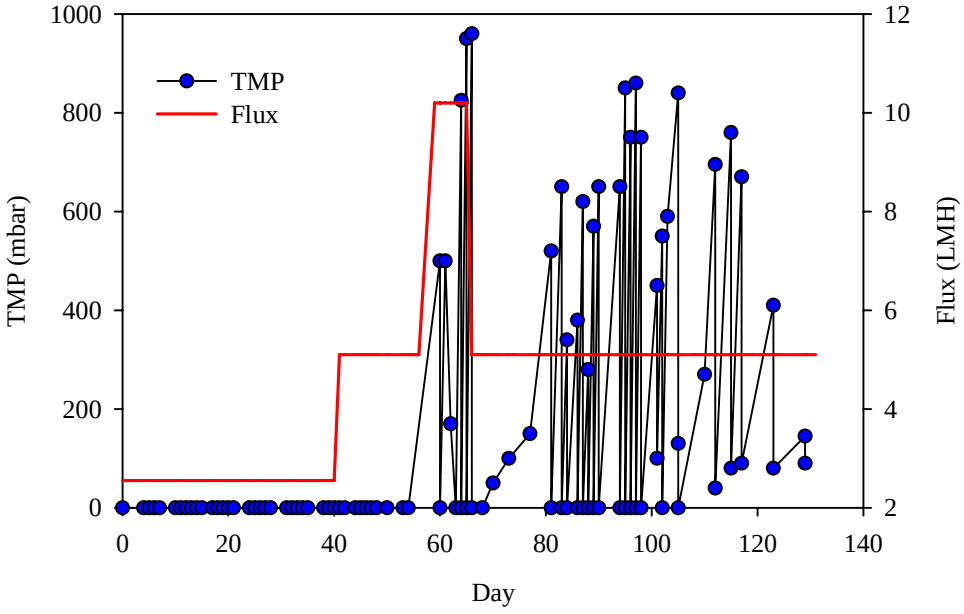

Fig. 4. Variations of TMP and flux in the CMBR

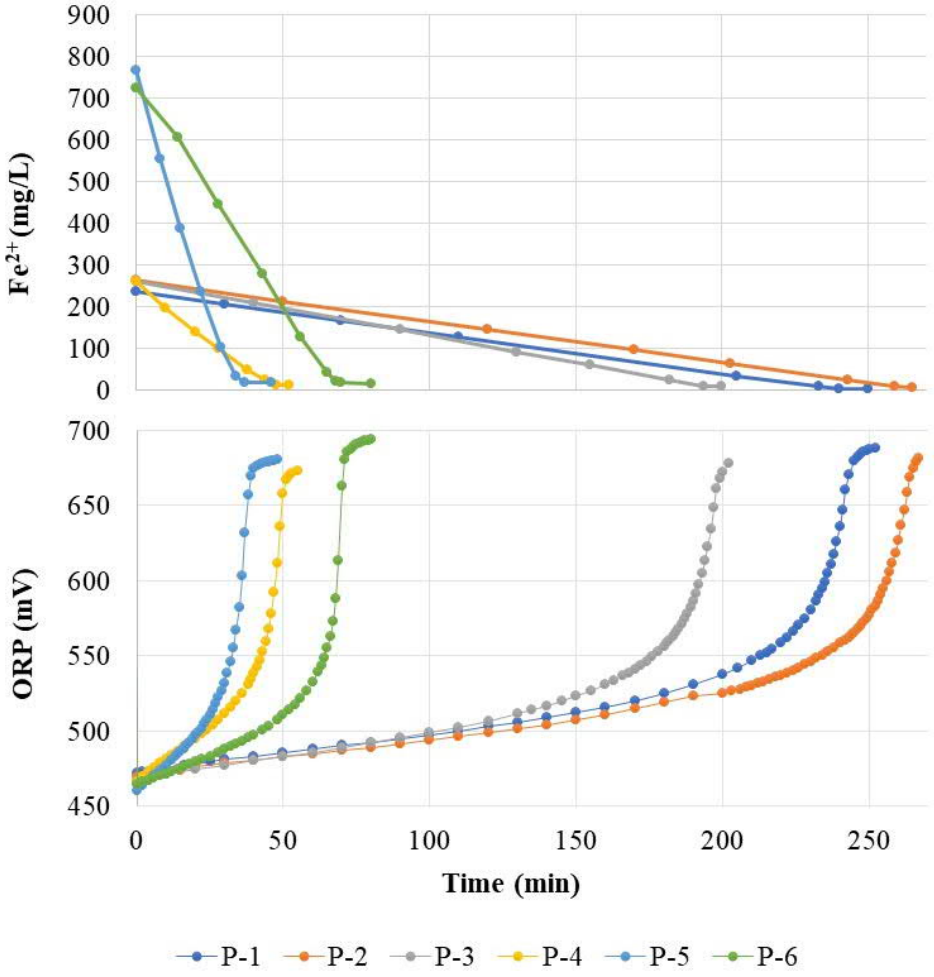

Fig. 5. Time course variations of Fe^{2+} (upper figure) and ORP (bottom figure) values in the batch operation of CMBR

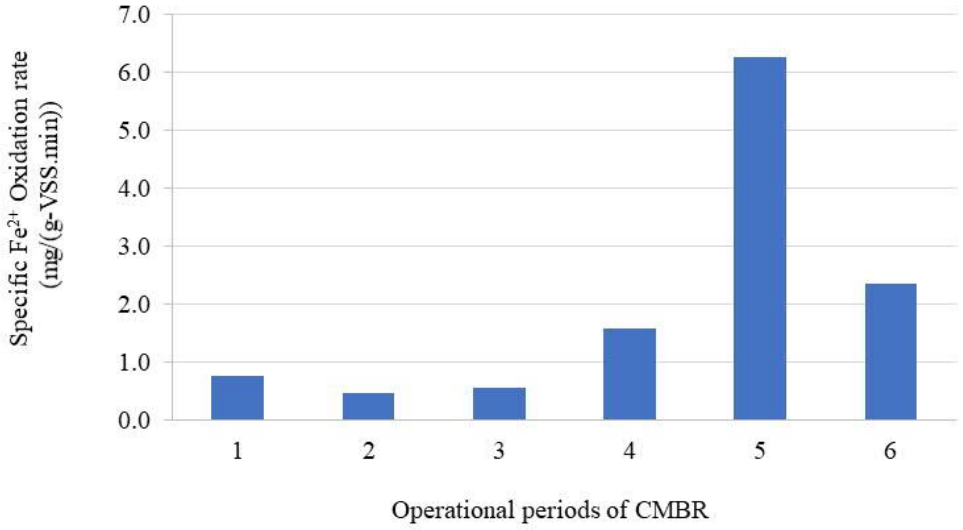

Fig. 6. Variation of specific Fe^{2+} oxidation rates observed in the batch cycles of CMBR operated under different periods (Table 2)

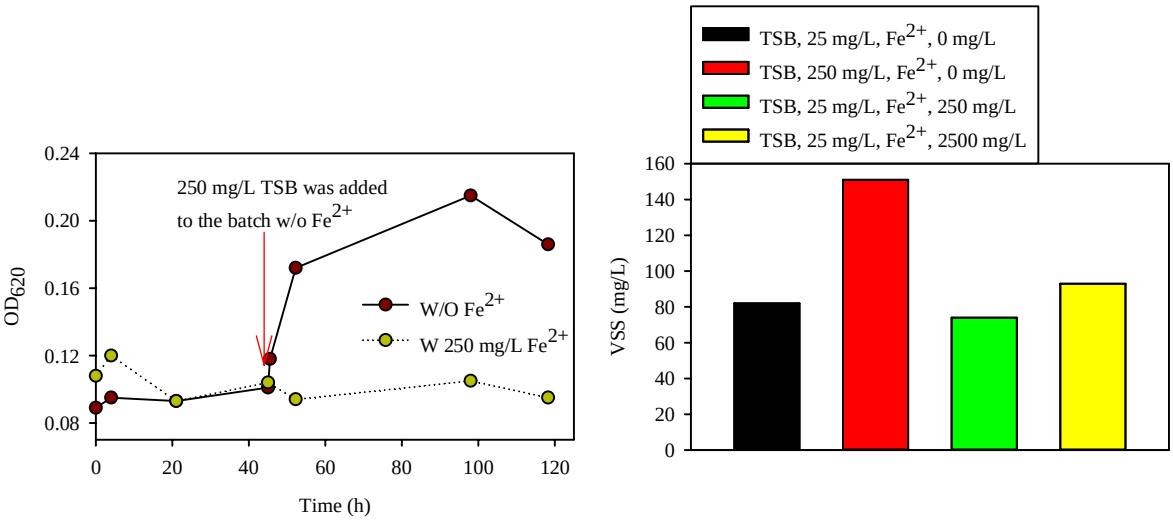

Fig. 7. Biomass growth in the presence and absence of Fe^{2+} (Batch-1 and -2) (left figure) and the final VSS concentrations under different batch conditions (right figure)

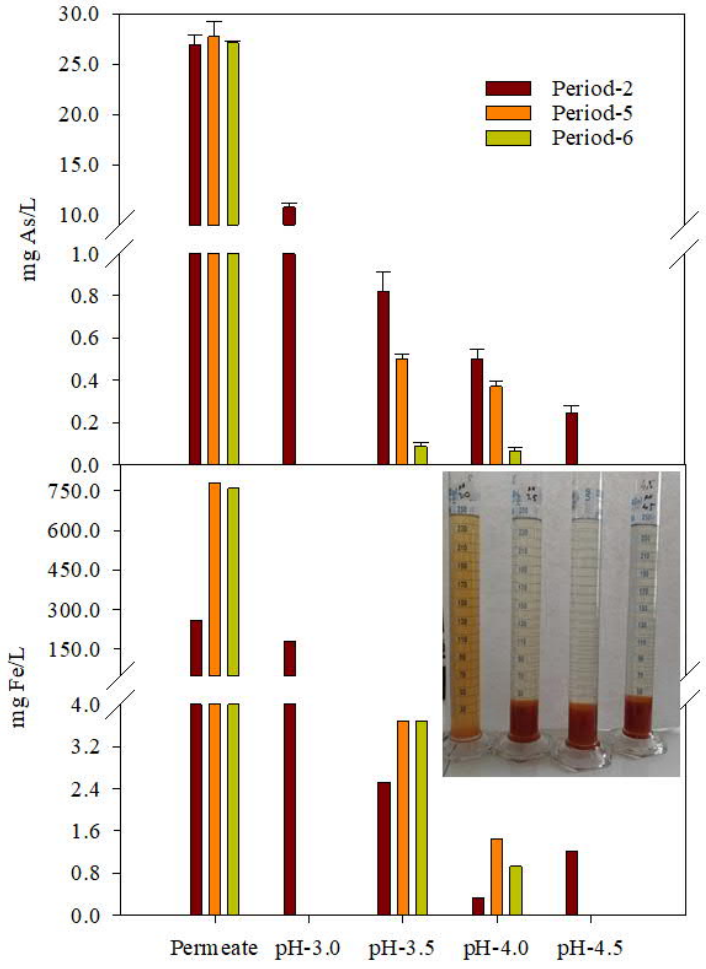

Fig. 8. Co-precipitation of iron and arsenic in the CMBR permeate at varying pHs. The inserted photograph illustrates the schwertmannite precipitation